Design in solid state chemistry based on phase homologies. Sb_4Te_3 and Sb_8Te_9 as new members of the series $(Sb_2Te_3)_m{\cdot}(Sb_2)_n$†

Pierre F. P. Poudeu and Mercouri G. Kanatzidis*

Received (in Cambridge, UK) 18th January 2005, Accepted 31st March 2005
First published as an Advance Article on the web 19th April 2005
DOI: 10.1039/b500695c

Sb_4Te_3 and Sb_8Te_9 are members of the homology $(Sb_2Te_3)_m{\cdot}(Sb_2)_n$, with structures consisting of Sb_2- and Sb_2Te_3-type slabs stacked along [001]; electrical conductivity and thermopower are reported for several members of this family.

Recently, we have highlighted the use of phase homologies for the prediction of new phases with predictable composition and structure.[1] This can be a powerful approach to designing new solid state compounds, especially where large homologies can be identified in which both the structural and compositional principles can be understood, as for example in $A_m[M_6Se_8]_m[M_{5+n}Se_{9+n}]$, $A_m[M_{1+l}Se_{2+l}]_{2m}[M_{1+2l+n}Se_{3+3l+n}]$ and $Cs_4[Bi_{2n+4}Te_{3n+6}]$.[2] The ability to access synthetically, and study experimentally and theoretically, successive members of a homology is a highly attractive proposition. It provides the possibility to understand structure–property relationships by making small but predictable changes in a well define structure–composition motif. The family of antimony tellurides with the general formula $(Sb_2Te_3)_m{\cdot}(Sb_2)_n$ has been recognized[3] to define a homologous series where Sb_2Te_3, Sb_2Te,[4] SbTe[5] and Sb_2 are structurally well characterized members. Considering that Sb_2Te_3 ($n = 0$) and Sb_2 ($m = 0$) (*i.e.* elemental antimony) are the two end members of the $(Sb_2Te_3)_m{\cdot}(Sb_2)_n$ family, intermediate members can be predicted by considering that individual slabs having the structure of antimony, Sb_2,[6] and slabs having the structure of Sb_2Te_3 (Fig. 1) are combined in various ratios (*i.e.* m/n) to form new structure types. Possible compositions and ordered stacking sequences of Sb_2Te_3 and Sb_2 based on the above assumption are Sb_4Te_3 (1/1, 2/2 and 3/3), Sb_2Te (1/2), SbTe (2/1), Sb_8Te_3 (1/3), Sb_8Te_9 (3/1), $Sb_{10}Te_6$ (2/3) and $Sb_{10}Te_9$ (3/2). According to the total number of slabs (Sb_2Te_3-type and Sb_2-type) in a stacking sequence, the cell parameters and the space group of each intermediate member can also be predicted. For instance, if the total number of slabs in a sequence is a multiple of three, only one set of the Sb_2Te_3/Sb_2 sequence is necessary to form a structure and the space group is $P\bar{3}m$, otherwise three sets of the Sb_2Te_3/Sb_2 sequence are needed and the space group is $R\bar{3}m$. All compounds of the $(Sb_2Te_3)_m{\cdot}(Sb_2)_n$ family have trigonal symmetry with similar a parameters (Table 1) while the c parameter is related to the total number of Sb_2Te_3-type (m) and Sb_2-type (n) slabs stacked along [0001] according to the equation $c_{(m,\,n)} = 1/3[m{\cdot}c' + n{\cdot}c'']$, c' and c'' being the c parameters of Sb_2Te_3 and Sb_2 respectively. The structures of $(Sb_2Te_3)_m{\cdot}(Sb_2)_n$ compounds can be differentiated only by the stacking pattern of Sb_2Te_3 and Sb_2 slabs (Fig. 1). Because of their similar *ab* planes these structures generate almost identical powder diffraction

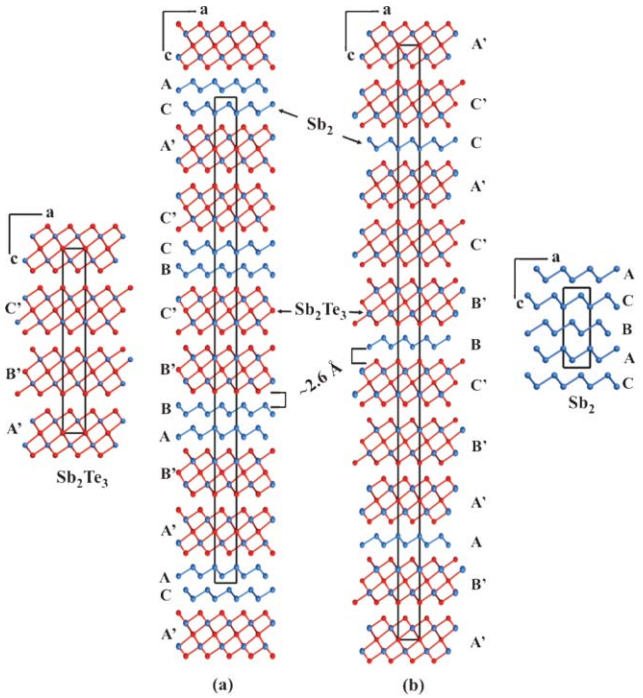

Fig. 1 Structures of (a) Sb_4Te_3 (42R) and (b) Sb_8Te_9 (51R) highlighting the stacking sequences of Sb_2Te_3 and Sb_2 slabs along [0001]. The structures of both end members of the $(Sb_2Te_3)_m{\cdot}(Sb_2)_n$ family are also shown. Blue spheres are Sb and red spheres are Te.

Table 1 Summary of crystallographic data for observed and predicted members of the $(Sb_2Te_3)_m{\cdot}(Sb_2)_n$ family

Formula	q[a]	m/n	Z	Space Group	a /Å	c/Å	c[b]/Å
Sb_2[7]	0/1	0/3	3	$R\bar{3}m$	4.307(1)	11.273(3)	—
Sb_8Te_3[c]	1/3	3/9	3	$R\bar{3}m$	4.28	—	64.28
Sb_2Te[5]	1/2	1/2	3	$P\bar{3}m$	4.272(1)	17.633(3)	17.668
Sb_4Te_3[d]	2/2[e]	6/6	6	$R\bar{3}m$	4.275(1)	83.564(2)	83.462
$Sb_{10}Te_6$[c]	2/3	6/9	3	$R\bar{3}m$	4.28	—	94.74
$Sb_{10}Te_9$[c]	3/2	9/6	3	$R\bar{3}m$	4.28	—	113.92
SbTe[6]	2/1	2/1	6	$P\bar{3}m$	4.26(1)	23.9 (3)	24.063
Sb_8Te_9[d]	3/1	9/3	3	$R\bar{3}m$	4.274(1)	102.69(9)	102.647
Sb_2Te_3[1]	1/0	3/0	3	$R\bar{3}m$	4.264(1)	30.458(1)	—

[a] q = Sb_2Te_3/Sb_2 stacking sequence. [b] Cell parameters calculated using the equation: $c = 1/3[m{\cdot}c' + n{\cdot}c'']$. [c] Predicted but still missing. [d] Present work. [e] 1 : 1 and 3 : 3 packing sequences are also possible for Sb_4Te_3.

† Electronic supplementary information (ESI) available: X-ray powder diffraction data and simulated precession photograph of Sb_4Te_3. See http://www.rsc.org/suppdata/cc/b5/b500695c/

*kanatzidis@chemistry.msu.edu

patterns (see ESI†) making single crystal analysis the best tool to clarify their details.

Given the above analysis, we started to investigate the crystal structures and transport properties (electrical conductivity and thermopower) of new members of the $(Sb_2Te_3)_m{\cdot}(Sb_2)_n$ family. Here we report the crystal structures and preliminary charge transport properties of Sb_4Te_3 and Sb_8Te_9, two new members of the $(Sb_2Te_3)_m{\cdot}(Sb_2)_n$ family.[7] Samples‡ used in our study were prepared starting from compositions calculated using the general formula. Single crystals of Sb_4Te_3 and Sb_8Te_9 used for the structure determination were selected from the reaction product.

Both compounds[8] as predicted by the homology crystallize in the trigonal space group $R\bar{3}m$ with very large c axes (Table 1). The deviation of the experimental value of the c parameter from that calculated using the above equation is less than 1% suggesting a distortion-free fitting of Sb_2Te_3 and Sb_2 building blocks in these structures. In the case of Sb_4Te_3, the analysis of diffraction data revealed a long c axis of 83.6 Å instead of 41.8 Å as might be expected by analogy to the structure of Bi_4Te_3.[9] In fact the structures of Sb_4Te_3 and Bi_4Te_3 are different. In Sb_4Te_3 (Fig. 1(a)), the Sb_2Te_3-type and Sb_2-type slabs alternate in pairs *i.e.* "two to two" (A′B′ABB′C′BCC′A′CA...) to form a structure with 42 atomic layers (42R). This generates a van der Waals gap between adjacent layers. In contrast, in Bi_4Te_3 the packing sequence involves the alternation of single Bi_2Te_3- and Bi_2-slabs, *i.e.* "one to one" (AA′BB′CC′…) which does not create a van der Waals gap in the structure. The "one to one" Bi_4Te_3-structure type for Sb_4Te_3 is yet to be found. As mentioned above, a "three to three" packing sequence (space group $P\bar{3}m$) can also be expected for this composition. The formation of a given structure type is strongly related to the details of the reaction conditions.

In the structure of Sb_8Te_9 (Fig. 1(b)), Sb_2Te_3-like and Sb_2-like slabs are arranged in the sequence "three to one" (A′B′C′BB′C′A′CC′A′B′A...) to form a structure with 51 atomic layers (51R). The gap between adjacent slabs (Sb_2Te_3 and Sb_2) is essentially the same in both structures (~2.6 Å). This value is intermediate to those found in the structures of Sb_2Te_3 (~2.8 Å) and elemental Sb (~2.3 Å) indicating the perfect additivity of Sb_2Te_3 and Sb_2 building blocks in the structures of $(Sb_2Te_3)_m{\cdot}(Sb_2)_n$ compounds.

The chemical bonding is similar in both structures. Within the two-layer slabs, the Sb–Sb bond is 2.909(1) Å in Sb_4Te_3 and 2.912(2) Å in Sb_8Te_9. These values are comparable to those found in Sb_2Te (2.902(1) Å) and SbTe (2.922(1) Å) but shorter than the value of 2.961 Å observed in elemental Sb. The Sb–Te bond distances range from 2.984(1) Å to 3.213(1) Å in Sb_4Te_3 and from 2.992(1) Å to 3.194(1) Å in Sb_8Te_9. Sb_4Te_3 belongs to the γ phase region of the Sb–Te binary phase diagram[10] while Sb_8Te_9 is completely out of the solid solution region at about 53 at% Te suggesting that the γ phase region may be broader than reported.

Preliminary thermopower and electrical conductivity measurements on oriented polycrystalline ingots of various members of the $(Sb_2Te_3)_m{\cdot}(Sb_2)_n$ family perpendicular to the c axis show positive values of the thermopower (p-type) (Fig. 2) indicating hole transport. The thermopower measured at 300 K ranges between 5 and 40 μV K^{-1}. These low values are consistent with the semimetallic character of $(Sb_2Te_3)_m{\cdot}(Sb_2)_n$ compounds. The "metallicity" of the compounds decreases as we move towards the Sb-poor region of the Sb–Te system. This is followed by an increase in the thermopower of the $(Sb_2Te_3)_m{\cdot}(Sb_2)_n$ compounds. This observation is in line with the value of 89 μV K^{-1} at room temperature[11] recently measured for pure Sb_2Te_3. All $(Sb_2Te_3)_m{\cdot}(Sb_2)_n$ samples showed very high electrical conductivities at room temperature with values of 6000 S cm^{-1} for Sb_8Te_9, 3000 S cm^{-1} for Sb_4Te_3, 3500 S cm^{-1} for SbTe and 1500 S cm^{-1} for Sb_2Te.

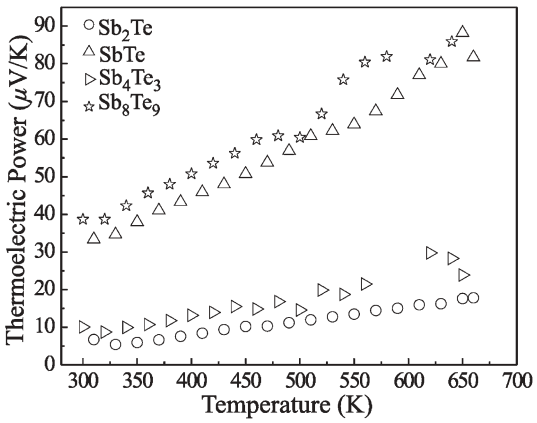

Fig. 2 Temperature dependence of the thermopower of known members of the $(Sb_2Te_3)_m{\cdot}(Sb_2)_n$ family.

In addition to the anisotropy in the electronic properties that is generally observed in compounds with layered structures, members of the $(Sb_2Te_3)_m{\cdot}(Sb_2)_n$ family are interesting because they represent an example of a natural superlattice structure. The superlattice is somewhat flexible as it can combine intimately a semi-conducting salt-like part (Sb_2Te_3) with a semi-metallic part (Sb_2) in various ratios. Controlling the ratio of the two substructures may allow a modulation of their electronic band structure and better control of the charge transport properties in this family of compounds.

Financial support from the Office of Naval Research is gratefully acknowledged.

Pierre F. P. Poudeu and Mercouri G. Kanatzidis*
Department of Chemistry, Michigan State University, East Lansing, MI 48824, USA. E-mail: kanatzidis@chemistry.msu.edu

Notes and references

‡ Crystals of Sb_4Te_3 and Sb_8Te_9 were obtained from reactions involving Sb and Te in the molar ratios 4 : 3 and 8 : 9 respectively. Polycrystalline single phase ingots of Sb_2Te, SbTe, Sb_4Te_3 and Sb_8Te_9 were obtained by reacting Sb and Te in the appropriate molar ratio. Approximately 10 g of the starting materials were vacuum-sealed in silica tubes and heated to 800 °C for 48 h during which time the furnace was allowed to rock 45° backwards and forwards (mixing). The furnace was then cooled to 500 °C in 24 h, annealed for 72 h and cooled to room temperature in 30 h. All phases (except Sb_2Te which melts congruently) melt incongruently around 540 °C (Shimadzu DTA-50).

Crystal data: Intensity data were collected using graphite monochromatized Mo Kα radiation on a STOE IPDS–II diffractometer for Sb_4Te_3 and a Siemens SMART Platform CCD diffractometer for Sb_8Te_9. Sb_4Te_3: trigonal, $R\bar{3}m$ (No. 166), a = 4.2754(6) Å, c = 83.5640(2) Å, V = 1322.8(4) $Å^3$, Z = 6, D_c = 6.551 g cm^{-3}, μ(Mo Kα) = 218 cm^{-1}, total reflections 4015, independent reflections 407 (R_{int} = 0.095), R_1 = 0.041, wR_2 = 0.106. Sb_8Te_9: trigonal, $R\bar{3}m$ (No. 166), a = 4.2738(5) Å, c = 102.689(9) Å, V = 1624.4(5) $Å^3$, Z = 3, D_c = 6.509 g cm^{-3}, μ(Mo Kα) = 217 cm^{-1}, total reflections 6155, independent reflections 623 (R_{int} = 0.047), R_1 = 0.029, wR_2 = 0.078. CCDC 261145 (Sb_4Te_3) and 261148 (Sb_8Te_9). See http://www.rsc.org/suppdata/cc/b5/b500695c/ for crystallographic data in CIF or other electronic format.

1 A. Mrotzek and M. G. Kanatzidis, *Acc. Chem. Res.*, 2003, **36**, 111–119.
2 M. G. Kanatzidis, *Acc. Chem. Res.*, 2005, in press (DOI: 10.1021/ar040176w).
3 L. E. Shelimova, O. G. Karpinskii, M. A. Kretova, V. I. Kosyakov, V. A. Shestakov, V. S. Zemskov and F. A. Kuznetsov, *Inorg. Mater.*, 2000, **36**, 768.
4 V. Agafonov, N. Rodier, R. Ceolin, R. Bellissent, C. Bergman and J. P. Gaspard, *Acta Crystallogr., Sect. C*, 1991, **C47**, 1141.
5 M. M. Stasova and O. G. Karpinskii, *Zh. Strukt. Khim.*, 1967, **8**, 654.
6 D. Schiferl, *Rev. Sci. Instrum.*, 1977, **48**, 24.
7 The compounds do not appear in the published binary Sb–Te phase diagram. F. Hulliger, Structural Chemistry of Layer-Type Phases, in *Physics and Chemistry of Materials with Layered Structures*, Reidel, Dordrecht, 1976, vol. 5, pp. 207–210; G. Ghosh, *J. Phase Equilib.*, 1994, **15**, 343.
8 The assignments of Te positions during the refinement of both structures were made by analogy with the structure of Sb_2Te_3 and bond valence sum (BVS) calculations. The BVS were 2.028, 2.046 and 1.989 for Te(1), Te(2) and Te(3) in Sb_4Te_3; 2.046, 2.052, 1.908, 2.076 and 1.935 for Te(1), Te(2), Te(3), Te(4) and Te(5) in Sb_8Te_9: N. E. Brese and M. O'Keeffe, *Acta Crystallogr., Sect. B*, 1991, **B47**, 192.
9 K. Yamana, K. Kihara and T. Matsumoto, *Acta Crystallogr., Sect. B*, 1979, **B35**, 147.
10 G. Ghosh, *J. Phase Equilib.*, 1994, **15**, 343; G. Ghosh, H. L. Lukas and L. Delaey, *Z. Metallkd.*, 1989, **80**, 731.
11 J. S. Dyck, W. Chen and C. Uher, *Phys. Rev. B*, 2002, **66**, 125206.

